Supplementary file SM4: Joint posterior distributions

CEA

The joint posterior distribution of tree lengths and rate multipliers resulting from the analysis of CEA under model C-Hom-14 are in SM4 Fig. 1 (above). The marginal posterior distribution of rate multipliers was strongly skewed to the left, with a median rate of ~1.9. Tree length density is concentrated around its median (~4.6) and comparable to those obtained under anatomical and PF schemes (SM4 Figs. 1b and 1c), although tree lengths were significantly longer than those obtained under either anatomical (one-tailed Komolgorov-Smirnov's $D=0.45$, $p << 0.001$) or PF ($D=0.89$, $p << 0.001$). The probability surface is better illustrated as a semi-log plot (see SM4 Fig. 2a). The overlap among rate multiplier distributions is evident in the marginal posterior, which is continuous and has fewer modes than partitions (n=8). Character segregation in the best model anatomical obtained under the anatomical partition scheme was poor, as shown by their quasi unimodal joint distribution (SM4 Figs. 1b). Median tree length was ~4.1 under this scheme. Under PF's best model, the marginal posterior of multipliers is clearly bimodal: the mass of the partition 1 is concentrated on the right peak, whereas the remaining densities are mixed in the left one (SM4 Figs. 1c). Tree length distribution was unimodal and symmetrical around the median (~3.6). As stated above, trees were significantly shorter than those obtained using C-Hom-14 and also shorter than those obtained under anatomical partitioning ($D=0.51$, $p << 0.001$). The joint posterior was scattered, but significantly less dispersed with respect to rate multipliers than C-Hom-14 (SM4 Figs. 1a).

OZL

The joint posterior density under homoplasy (SM4 Figs. 1d) was also highly skewed with respect to the multipliers, as observed for CEA (SM4 Figs. 1a). When displayed as a semi-log plot (SM4 Figs. 1b), the number of modes in the marginal multiplier distribution was significantly smaller than the number of partitions and the strong overlap among the mid-range multipliers is expressed in the highest mode. High-end multiplier values make up a discrete mode to the right, but like in the case of CEA, correspond to a small fraction of the posterior.

Like CEA (SM4 Figs. 1b) the joint posterior of tree lengths and rates under anatomical partition of OZL (SM4 Figs. 1e) had no discrete modes, but it was more scattered, reflecting the higher rate variation in this matrix.

When plotted in linear scale, the marginal multiplier posterior under PF's bes model was also highly skewed and clearly multimodal (SM4 Figs. 1f). In log scale, it revealed four discrete modes, but most of its density was concentrated around 1, as reflected by the joint probability surface (SM4 Fig. 2c). The multiplier posterior was far less aggregated than in the case of O-Hom-14 (SM4 Fig. 2b), but the smaller modes made up a much reduced fraction of the joint posterior. The marginal distribution of tree lengths was continuous, but jagged with multiple peaks (SM4 Fig. 2c), as opposed to the smoother density obtained under homoplasy partitioning (SM4 Fig. 2b). There was significantly shortening of trees between homoplasy and anatomy ($D=0.22$, $p << 0.001$), homoplasy and PF ($D=0.11$, $p << 0.001$) and PF vs. anatomy ($D=0.12$, $p << 0.001$). Although significant, the increasing effect of partitioning on median tree length was under 2% in every case, as opposed to 12-28% in CEA.

SCO

Joint posterior of tree lengths and rates (SM4 Figs. 1g) also resembled surfaces for CEA and OZL (SM4 Figs. 1a and 1d) and likewise, it is better shown on as a semi-log plot (SM4 Fig. 2d). Once again, the joint density was scattered, the marginal rate multiplier posterior was continuous and has fewer modes than partitions, while the marginal tree length distribution appeared unimodal.

The joint posterior of tree length and rates under PF was scattered and almost continuous, but oddly truncated around a rate value of 2 (SM4 Figs. 1h). Because the top model under anatomical partitioning used fixed branch lengths and equal rates, there were no comparable results to be shown.

With respect to branch lengths, homoplasy partitioning more than doubled the median tree length (from ~3.1 to 6.4) if compared to S-Unp-6 ($D=0.98$, $p << 0.001$). The large difference arises because the model employs $\lambda=5$ as opposed to 10, as most other best models.

SM4 Figure 1. Heatmaps of joint posterior distributions representing tree length variation as a function of APRV (rate multipliers) or ACRV (character rates). Marginal densities are represented by the smoothed histograms on top and to the right of each heatmap, with 95% HPD highlighted in red. a) C-Hom-14 b) C-Ana1-34 c) C-Parfin2-14 d) O-Hom-14 e) O-Ana-10 f) O-ParFin-18 g) S-Hom-13 h) O-ParFin8-18.

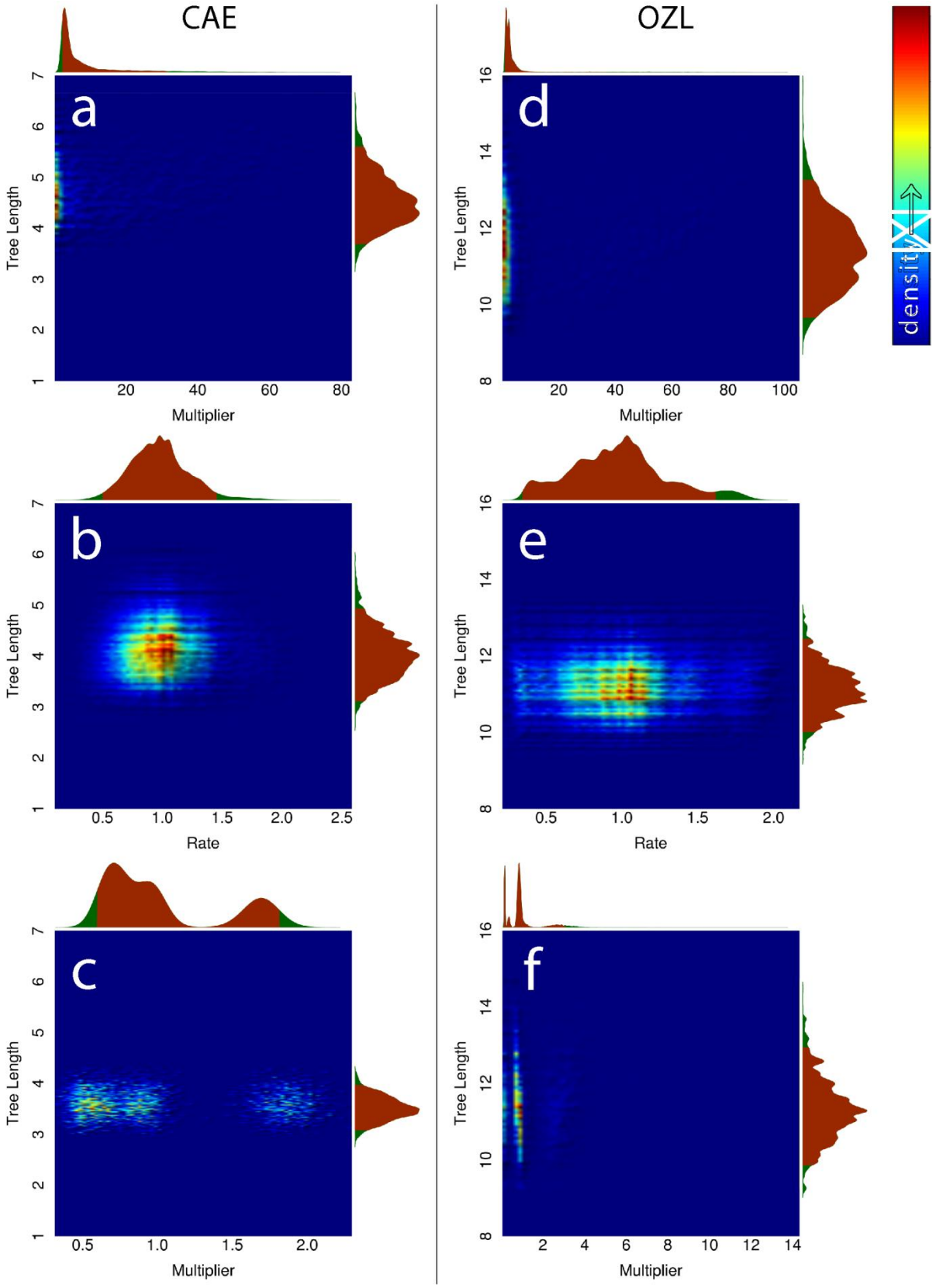

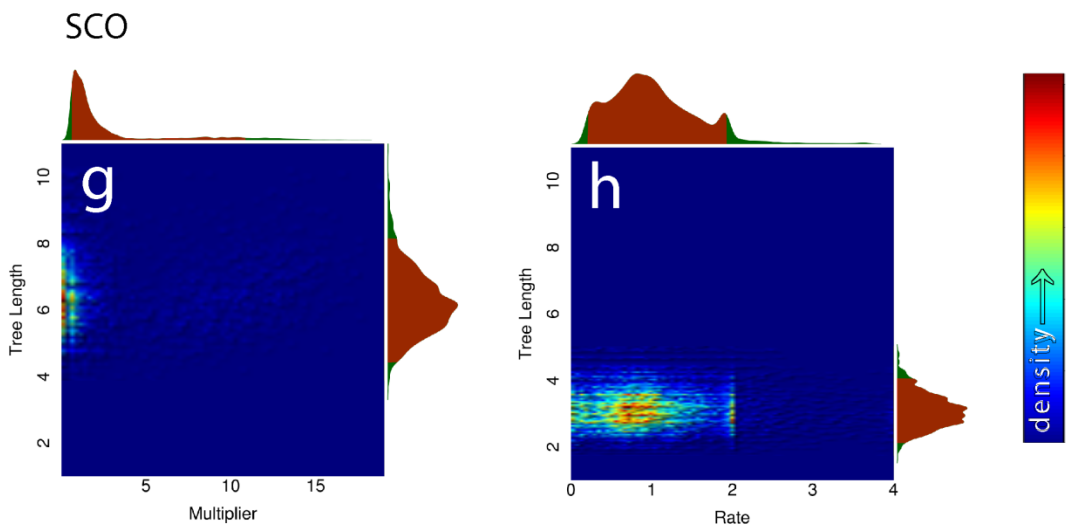

SM4 Figure 2. Joint posterior distributions of tree lengths and rate multipliers represented as semi-log plots (y-axis in linear and x-axis in log scale). a. C-Hom-14. b. O-Hom-14. c. OParFin2-18. d. S-Hom-13.